HHS Public Access

Author manuscript

J Endocrinol. Author manuscript; available in PMC 2016 October 01.

Published in final edited form as:

J Endocrinol. 2015 November ; 227(2): 93–103. doi:10.1530/JOE-15-0284.

Glucagon receptor inactivation leads to α-cell hyperplasia in zebrafish

Mingyu Li[1], **E Danielle Dean**[2], **Liyuan Zhao**[1,3], **Wendell E. Nicholson**[2], **Alvin C. Powers**[1,2,4], and **Wenbiao Chen**[1]

[1]Departments of Molecular Physiology and Biophysics, Vanderbilt University School of Medicine, Nashville, TN 37232

[2]Division of Diabetes, Endocrinology, and Metabolism, Department of Medicine, Vanderbilt University, Nashville, TN 37232

[3]Third Institute of Oceanography, State Oceanic Administration, Xiamen 361005, China

[4]Veterans Affairs Tennessee Valley Healthcare System, Nashville, TN 37212

Abstract

Glucagon antagonism is a potential treatment for diabetes. One potential side effect is α-cell hyperplasia, which has been noted in several approaches to antagonize glucagon action. To investigate the molecular mechanism of the α-cell hyperplasia and to identify the responsible factor, we created a zebrafish model in which glucagon receptor (gcgr) signaling has been interrupted. The genetically and chemically tractable zebrafish, which provides a robust discovery platform, has two glucagon receptor genes (*gcgra* and *gcgrb*) in its genome. Sequence, phylogenetic, and synteny analyses suggest that these are co-orthologs of the human *GCGR*. Similar to its mammalian counterparts, *gcgra* and *gcgrb* are mainly expressed in the liver. We inactivated the zebrafish *gcgra* and *gcgrb* using TALEN (Transcription activator-like effector nuclease) first individually and then both genes, and assessed the number of α-cells using an α-cell reporter line, *Tg(gcga:GFP)*. Compared to wild-type fish at 7 days postfertilization, there were more α-cells in *gcgra−/−*, *gcgrb−/−*, and *gcgra−/−;gcgrb−/−* fish and there was an increased rate of α-cell proliferation in the *gcgra−/−; gcgrb−/−* fish. Glucagon levels were higher but free glucose levels were lower in *gcgra−/−*, *gcgrb−/−*, and *gcgra−/−;gcgrb−/−* fish, similar to *Gcgr−/−* mice. These results indicate that the compensatory α-cell hyperplasia in response to interruption of glucagon signaling is conserved in zebrafish. The robust α-cell hyperplasia in *gcgra−/−;gcgrb−/−* larvae provides a platform to screen for chemical and genetic suppressors, and ultimately to identify the stimulus of α-cell hyperplasia and its signaling mechanism.

Corresponding author and person to whom reprints should be addressed: Wenbiao Chen, Department of Molecular Physiology and Biophysics, Vanderbilt University School of Medicine, Light Hall, Room 711, 2215 Garland Ave, Nashville, TN 37232, Phone: (615) 936-8126, Fax: (615) 322-7236, wenbiao.chen@vanderbilt.edu.

Declaration of interest

The authors have nothing to disclose.

Author contribution

W.C is the guarantor of this work and, as such, had full access to all of the data in the study and takes responsibility for the integrity of the data and the accuracy of the data analysis. WC, ML, DD, and ACP designed the study. ML, EDD, LZ and WEN performed the key experiments. WC, ML, DD, ACP, LZ and WEN participated in the planning of the work and the interpretation of the results. ML and WC drafted the manuscript. WC, ML, DD, and ACP have participated in the revising of the paper.

Keywords

Cell growth control; Glucagon; Mutations; Fish; Whole animal physiology

Introduction

Glucagon is a peptide hormone secreted by pancreatic α-cells. It is the main counter-regulatory hormone of insulin. Glucagon acts primarily on liver through glucagon receptor (GCGR) to regulate hepatic glucose production (Mayo, et al. 2003). The GCGR is a class B G-protein-coupled receptor that couples to Gs (G protein subunits) and activates adenylate cyclase to increase intracellular levels of cAMP upon ligand binding (Brubaker and Drucker 2002). The cAMP subsequently activates protein kinase A (PKA), leading to increased glycogenolysis and gluconeogenesis and decreased glycogen synthesis (Jiang and Zhang 2003). GCGR is primarily expressed in the liver, but is also detected in other tissues, including β-cells, heart, intestinal smooth muscle, kidney, brain, and adipose tissue (Ali and Drucker 2009; Hansen, et al. 1995; Kedees, et al. 2009). Gcgr expression in hepatocytes is upregulated by glucose and factors known to raise intracellular cAMP levels (Abrahamsen, et al. 1995).

Glucagon raises the blood glucose and excess glucagon action is seen in both type 1 and type 2 diabetes (Lund, et al. 2014). Knockout of Gcgr in mice results in mild hypoglycemia and decreased adiposity, and prevents diabetes induced either by streptozotocin or by a high fat diet (Conarello, et al. 2007; Gelling, et al. 2003; Lee, et al. 2011), supporting glucagon antagonism as a potential treatment for both types of diabetes. However, as compensation to loss of glucagon action, *Gcgr*−/− mice also exhibit α-cell and δ-cell hyperplasia, hyperglucagonemia (Gelling et al. 2003), and may develop pancreatic endocrine tumors (Gelling et al. 2003; Yu, et al. 2011). Similarly, loss of GCGR function in humans is associated with hyperglucagonemia, α-cell hyperplasia and endocrine tumor (Zhou, et al. 2009). These undesirable consequences of glucagon antagonism must be mitigated if anti-glucagon treatment is to be useful and safe. A key question about the compensatory α-cell hyperplasia is the responsible mechanism. Liver-specific inactivation of Gcgr or its downstream transducer Gsα (G_s alpha subunit) in mice results in similar phenotype, suggesting the signal originates in the liver (Chen, et al. 2005; Longuet, et al. 2013). Furthermore, α-cell hyperplasia occurs in islets transplanted beneath the renal capsule, indicating the responsible factor circulates (Longuet et al. 2013). However, neither the factor that stimulates α-cell hyperplasia nor its signaling mechanism is known.

The zebrafish has emerged as a discovery platform for understanding molecular mechanisms of vertebrate biology. Its small size and transparent larvae make zebrafish an extremely useful for genetic and chemical modifier screens to discover critical components of a biological process (Lieschke and Currie 2007). Many signaling pathways and transcription factors important for mammalian pancreatic α-cell and β-cell development are conserved in zebrafish (Biemar, et al. 2001; Field, et al. 2003; Hesselson, et al. 2011; Maddison and Chen 2012). Here we investigated the biology of the glucagon system in zebrafish in an effort to determine if the zebrafish might serve as a discovery platform for signals and mechanisms

that regulate α-cell mass. We found that zebrafish have two *gcgr* genes, *gcgra* and *gcgrb*. We functionally characterized their gene products, and found that α-cells hyperplasia occurs in *gcgra*-and/or *gcgrb*-deficient zebrafish larvae.

Materials and Methods

Zebrafish lines and maintenance

Zebrafish (Danio rerio) were raised in an Aquatic-Habitats system on a 14:10-h light-dark cycle at 28°C. Embryos were obtained by natural cross and kept in embryo rearing solution and staged according to standard methods (Kimmel, et al. 1995). In this study, *Tg(gcga:GFP)*(Zecchin, et al. 2007) was used to mark α-cells. All procedures have been approved by the Vanderbilt University Institutional Animal Care and Use Committee.

TALEN-mediated mutagenesis of *gcgra and gcgrb*

The candidate TALEN (Transcription activator-like effector nuclease) target sequences of *gcgra* and *gcgrb* were identified online using TALEN Targeter (https://tale-nt.cac.cornell.edu/). The target sequences for the *gcgra* TALEN pair are 5′-GCCCTGCCCAACACTACAGT-3′ (left) and 5′-GTATCTGCCCTGGCACAAGG-3′ (right). The target sequences for the *gcgrb* TALEN pair are 5′-CTTCTGGGAAATCTCTGAAG-3′ (left) and 5′-TGGAGGATCTACACCAATG-3′ (right). The TALENs were assembled using “Golden Gate TALEN assembly” kit (Cermak, et al. 2011). TALEN expression vectors were linearized and used as template for capped mRNA synthesis uing T3 mMessage mMachine Transcription Kit (Ambion, USA) according to the manufacturer’s instructions. Equal amounts of capped mRNAs were mixed and co-injected into one-cell stage zebrafish embryos at the dose of 200pg/embryo. T7 Endonuclease I (NEB, USA) digestion was used to evaluate the efficiency of the TALENs. Briefly, a ~400 bp fragment was amplified from genomic DNA isolated from injected-embryos at 24 hours postfertilization (hpf), and purified product was digested and cleaved products resolved from intact products by agarose gel electrophoresis.

A *gcgra* allele with 22 bp deletion, designated as $gcgra^{vu600}$ and a *gcgrb* allele with 1 bp deletion, designated as $gcgrb^{vu601}$, were selected for additional analysis. For $gcgra^{vu600}$ carriers, PCR products amplified using gcgra-Mu22-F1 and gcgra-TN2-GTR following gel electrophoresis with 4% NuSieve GTG agrose (Lonza, ME) to distinguish the WT (180 bp) and mutant (158bp) (Fig. 3G). For $gcgrb^{vu601}$ carrriers, PCR products amplified using gcgrb-TN2-GTF and gcgrb-TN2-GTR were digested with PstI. PCR product from carriers could not be digested (Fig. 3H).

Cloning and sequence analysis

A putative *gcgra* gene was identified in Ensembl (http://www.ensembl.org)(Ensembl ID: ENSDART00000156788). A pair of primers, gcgra-Long-F1 and gcgra-Long-R1, was used to amplify the entire open reading frame (ORF) from zebrafish cDNA using Q5 High-Fidelity DNA Polymerase (NEB). To obtain the ORF of *gcgrb*, the cDNA sequence was first determined using 3′- and 5′-RACE based on the ensemble ID ENSDART00000021878. The entire ORF was subsequently cloned using primers gcgrb-Long-F1 and gcgrb-Long-R1.

Phylogenetic analysis was performed by the neighbor-joining method using the MEGA 4 software (The Biodesign Institute, Tempe, AZ) and full-length amino acid sequences. Bootstrap analyses were run on 1,000 replicates. The genomic structure of zebrafish *gcgra* and *gcgrb* was determined by the Blat program (http://genome.ucsc.edu/cgi-bin/hgBlat) using the cloned full-length cDNA sequence as query to search zebrafish Assembly Zv9 (July 2010). Synteny analysis was carried out based on zebrafish Assembly Zv9 (http://www.ensembl.org/Danio_rerio/Info/Index) and human Build GRCh38 (http://www.ensembl.org/Homo_sapiens/index.html), and from zebrafish and human synteny map, respectively.

RNA extraction, RT-PCR and Quantitative real-time RT-PCR (qRT-PCR)

Total RNA was isolated from adult zebrafish and embryos using TRIzol reagent (Invitrogen Life Technologies, CA) and digested by the RQ1 RNase-Free Dnase (Promega, WI) to remove any genomic DNA contamination. First strand cDNA was synthesized using M-MLV (Promega, WI) with oligo$(dT)_{16}$ as primer. RT-PCR was carried out using GoTaq Flexi DNA polymerase (Promega, WI) at MyCycler Thermal Cycler (Bio-Rad, Hercules, CA). The primers are listed in Supplemental Table 1. *β-actin* was used as an internal control. RT-PCR products were fractionated by 1.5% agarose gel electrophoresis, stained with ethidium bromide, and photographed using ChemiDoc XRS Gel Documentation system (Bio-Rad, Hercules, CA). qRT-PCR was performed in a CFX96 system (Bio-Rad, Hercules, CA). After a 3-min incubation at 95°C, the amplification was performed as follows: 95°C, 10 s; 60°C, 30 s, for 40 cycles. Each assay for an unknown sample was performed in triplicate. mRNA levels were calculated using $2^{-\Delta\Delta Ct}$ method (Livak and Schmittgen 2001) and presented as relative (fold) levels normalized to the level of *β-actin*.

cAMP accumulation

Zebrafish glucagon, Gcga (HSEGTFSNDYSKYLETRRAQDFVQWLMNA) and Gcgb (HSEGTFSNDYSKYLETRRAQDFVQWLMNS) peptides were synthesized by GENEWIZ (GENEWIZ, MA). Mouse glucagon was from Sigma-Aldrich (Sigma G2044). ORF of zebrafish *gcgra* and *gcgrb* were subcloned in the pcDNA 3.1+ at Kpn I and EcoR I sites. Mouse *Gcgr* ORF was subcloned in the pcDNA 3.1+ at EcoR I and Xho I sites. HEK293T cells are co-transfected with CRE-luciferase reporter plasmid and pcDNA3.1, pcDNA3.1-*gcgra*, pcDNA3.1-*gcgrb*, pcDNA3.1-*Gcgr* using Dilute LipoD393™ (SignaGen Laboratories). Twenty-four hours after transfection, cells were washed and dissociated, then evenly seeded into each well of a 96-well plate. Different final concentrations of glucagon peptides were added to each well with Forskolin as the control. After a 4-hours incubation at 37°C, ONE-Glo™ Luciferase mixture was added to each well. After a 5-minute incubation at room temperature, signal in the plate was read using SpectraMax M5 Microplate Reader (Molecular Devices). Nonlinear regression analysis was performed to calculate cAMP concentrations using GraphPad Prism software (GraphPad Software Inc., CA).

Free glucose assay

Free glucose of zebrafish larvae was determined using the Amplex Red Glucose/Glucose Oxidase Assay Kit (Life Technologies, USA). A pool of 10 larvae was homogenized in 100

μl of sample buffer. The homogenate was cleared by centrifugation. 10 μl of supernatant (equivalent of one larva) was measured according to the manufacturer's instructions. The reaction was incubated for 30 minutes at room temperature and fluorescence was measured at Ex/Em = 535/590 nm in a SpectraMax M5 Microplate Reader (Molecular Devices). At least three 10-fish pools of each genotype were measured.

Whole mount in situ hybridization and whole mount immunofluorescence

Digoxigenin (DIG)-labeled antisense and sense RNA probes were synthesized in vitro using the linearized plasmid as template. Hybridization was carried out as described previously (Ni, et al. 2012). The larval zebrafish of *Tg(gcga:GFP)* were stained using monoclonal anti-glucagon antibody (Sigma G2654) using standard techniques as described previously (Li, et al. 2014).

Proliferation analysis

Proliferation was analyzed using the Click-iT EdU Alexa Fluor 594 Imaging Kit (C10339; Invitrogen). To identify proliferating α-cell, embryos were incubated with 1 mmol/l 5-ethynyl-2-deoxyuridine (EdU) for 24 hours starting at 4 days postfertilization (dpf). EdU was detected according to published protocols (Li, et al. 2013). All images were collected using a Zeiss LSM710 (Carl Zeiss).

Counting of α-cells

After fixation in 4% paraformaldehyde overnight at 4°C, larvae were washed with 1x PBS plus 0.1% Tween-20 (PBST) and flat mounted in Aqua-Mount (Richard-Allan Scientific) with their right side facing the coverslip. The larvae were flattened just to disrupt the islet slightly to allow better resolution of α-cell. The α-cells were counted according to the GFP signal using a Zeiss AxioImager under a 40x lens or using confocal projections taken by Zeiss LSM510 under a 40x lens (Carl Zeiss).

Whole fish glucagon content measurement

Glucagon content in zebrafish was measured by radioimmunoassay (RIA) in the Vanderbilt Hormone Assay Core similarly to mouse whole pancreata measurements (Longuet et al. 2013). The two zebrafish peptides share 76% identity with mammalian glucagon. Ten zebrafish larvae (7 dpf) were collected in 0.11N HCL in water and homogenized with a Kontes motorized homogenizer and pestle. The samples were solubilized for 72 hours at 4°C while rotating. Cleared extracts were stored at −80°C after centrifugation until use. We used a glucagon RIA kit (Siemens #KGND1) according to the manufacturer's protocol with modifications to increase the sensitivity. Specifically, the glucagon antibody was diluted two-fold and the glucagon I^{125} diluted to 5000 cpm per tube. The antibody detected the two zebrafish peptides with equal affinity, albeit with a small reduction (right shift) compared to the mammalian peptide (Data not shown). There was no difference in the slope of the binding curve between mammalian, zebrafish a, or zebrafish b glucagon ($P>0.05$).

Statistics

Data are means and standard errors. Data were analyzed by one-way ANOVA followed by Newman-Keuls post hoc test or t-test (SPSS, Chicago, IL). Significance was accepted at $P < 0.05$.

Results

Cloning and characterization of two gcgr genes from Zebrafish

Two putative *gcgr* genes were found in Ensembl zebrafish genome assembly (http://www.ensembl.org/Danio_rerio/Info/Index). Subsequently, primers were designed to amplify both ORFs. The ORF of *gcgra and gcgrb* were 1563 and 1527 bp and encoding proteins of 520 and 508 amino acids, respectively. Structural analysis revealed that both zebrafish *gcgra* and *gcgrb* had a structure similar to their mammalian counterparts, which contained an extracellular domain (ECD), seven transmembrane domains (7TM), and an intracellular domain (ICD).

We next generated a phylogenetic tree using the neighbor-joining method. As shown in Figure 1A, zebrafish Gcgr forms a cluster with known GCGRs with a high bootstrap support value and well separated from GIP receptors, GLP1 receptors and GLP2 receptors. Synteny analysis revealed that zebrafish *gcgra* is located on Chromosome 3, *gcgrb* is located on Chromosome 1, while the human *GCGR* locus is on Chromosome 17. To explore the possible synteny relationship between zebrafish *gcgr* and human *GCGR*, we compared genes surrounding the *GCGR* loci. Several neighboring genes of *GCGR*, namely *BAIAP2*, *AATK*, *SLC25A10*, *FN3KRP*, *TBCD*, *ZNF750*, *B3GNTL1* and *METRNL*, also had their orthologs near zebrafish *gcgra* or *gcgrb* (Figure 1B). This conserved synteny relationship provides further evidence that *gcgra* and *gcgrb* are both orthologous to human *GCGR*.

Expression patterns of gcgra and gcgrb mRNA

RT-PCR detected *gcgra* and *gcgrb* mRNA in all stages examined, including 1 dpf, 2 dpf, 3 dpf, 5 dpf, 7 dpf and 3-weeks of age (Figure 2A). In adult tissues, *gcgra* mRNA was most abundant in liver, followed by brain, muscle and heart, but was undetectable in intestines. Similarly, *gcgrb* mRNA was most abundant in liver, but was also expressed in intestines at a level similar to brain and was undetectable in muscle and heart. Therefore, *gcgra* and *gcgrb* have distinctive expression in muscle, heart and intestines (Figure 2B).

Functional Characterization of zebrafish Gcgra and Gcgrb

There are two glucagon genes in zebrafish, *gcga* and *gcgb* (Argenton, et al. 1999; Cruz, et al. 2010). We synthesized Gcga and Gcgb peptides and determined their dose response curve in HEK293T cells expressing Gcgra, Gcgrb and mouse GCGR using the CRE-luc reporter system. As shown in Figure 2, zebrafish Gcga and Gcgb stimulated cAMP accumulation in cells expressing zebrafish Gcgra with EC50 value of 4.16 nM and 14.6 nM, respectively. Mouse GCG had a much higher (1.96 μM) EC50 on zebrafish Gcgra (Figure 2C and Table 1). The mouse and two zebrafish glucagon peptides activated zebrafish Gcgrb at similar EC50 values (Gcga, 27.95 nM; Gcgb, 14.88 nM; and GCG, 40.46 nM) (Figure 2D and Table 1). However, Gcga and Gcgb only weakly activated mouse GCGR, contrasting to

an EC50 value of 8.33 nM for mouse GCG. These data suggested that the two zebrafish glucagon receptors have similar characteristic in responding to zebrafish glucagons (Gcga and Gcgb), but only Gcgrb responds to mouse glucagon. Zebrafish glucagons have a limited activity on the murine GCGR.

Generation of *gcgra* and *gcgrb* mutations using TALEN

To investigate the physiological function of Gcgra and Gcgrb, we generated loss-of-function alleles of *gcgra* and *gcgrb* using TALEN-mediated mutagenesis. The TALENs targeted the 3rd exon of *gcgra* and 2nd exon of *gcgrb*, respectively. From the TALEN mRNA-injected founders, we obtained one germline mutations in *gcgra* with a 22 bp deletion (*gcgra*^{vu600}), and one germline mutation in *gcgrb* with 1bp deletion (*gcgrb*^{vu601}), both resulting in reading-frame shift and premature stop codon (Figure 3A–H). qRT-PCR analysis showed that *gcgra* mRNA levels were not changed in the *gcgrb*^{vu601}/*gcgrb*^{vu601} mutants, but were decreased in *gcgra*^{vu600}/*gcgra*^{vu600}(0.65 ± 0.02) and *gcgra*^{vu600}/*gcgra*^{vu600}; *gcgrb*^{vu601}/*gcgrb*^{vu601} (0.55 ± 0.02). The levels of *gcgrb* mRNA also were not changed in the *gcgra*^{vu600}/*gcgra*^{vu600} mutants, but were decreased in *gcgrb*^{vu601}/*gcgrb*^{vu601} mutants (0.67 ± 0.05) and *gcgra*^{vu600}/*gcgra*^{vu600}; *gcgrb*^{vu601}/*gcgrb*^{vu601} mutants (0.56 ± 0.16) (Figure 3I). The results suggest that there is no compensatory regulation of the two *glucagon* genes. The reduction of the mutant mRNA levels is likely due to nonsense-mediated decay of mRNA.

Disruption of zebrafish *gcgra* and *gcgrb* causes pancreatic α-cell hyperplasia in larvae

To determine the role of glucagon receptors in the regulation of pancreatic α-cell mass, we crossed the *gcgra*^{vu600} *and gcgrb*^{vu601} into *Tg(gcga:GFP)* fish whose α-cells are labeled with GFP (Zecchin et al. 2007), allowing cell number determination. We confirmed by immunofluorescence that all GFP positive cells in the islet of the transgenic fish express Glucagon (Supplemental Fig. 1). We then determined the number of α-cells in wild-type and mutants at 7 dpf. Compared to *Tg(gcga:GFP)* with wild-type *gcgr* genes (20.63 ± 0.53; mean ± SE), there was an increase of α-cell number in the principal islet of *gcgra*^{vu600}/*gcgra*^{vu600}; *Tg(gcga:GFP)* (27.73 ± 1.50; P<0.01)) and *gcgrb*^{vu601}/*gcgrb*^{vu601}; *Tg(gcga:GFP)* (23.64 ±0.54; P< 0.01)(Figure 4A and 4B). There increase was even greater in *gcgra*^{vu600}/*gcgra*^{vu600}; *gcgrb*^{vu601}/*gcgrb*^{vu601}; *Tg(gcga:GFP)* fish (32.89 ± 0.84; P< 0.001) (Figure 4A and 4B). To determine when the difference occurs, we followed α-cell number from 3 dpf to 8 dpf in *Tg(gcga:GFP)* and *gcgra*^{vu600}/*gcgra*^{vu600}; *gcgrb*^{vu601}/*gcgrb*^{vu601}; *Tg(gcga:GFP)* fish. The increase of α-cell number was observed as early as 4 dpf (19.38 ± 0.65 vs. 25.00 ± 0.96, P< 0.001) (Figure 4C). The largest single-day increase of α-cells occurred from 4 dpf to 5 dpf in *gcgra*^{vu600}/*gcgra*^{vu600}; *gcgrb*^{vu601}/*gcgrb*^{vu601}; *Tg(gcga:GFP)* fish (Figure 4C). These data suggest that disruption of zebrafish *gcgra* and *gcgrb* causes supernumerary α-cells in zebrafish.

To determine whether α-cell replication contributed to the supernumerary α-cells in zebrafish glucagon receptor mutants, we incubated 4 dpf larvae with EdU for 24 hours to label replicating cells. Compared to *Tg(gcga:GFP)* (1.71 ± 0.56), there were a significant increase of EdU positive α-cells in *gcgra*^{vu600}/*gcgra*^{vu600}; *gcgrb*^{vu601}/*gcgrb*^{vu601};*Tg(gcga:GFP)* (4.56+0.99; P<0.05) (Figure 5). The number of EdU positive α-cells trended to be increased in both *gcgra*^{vu600}/*gcgra*^{vu600}; *Tg(gcga:GFP)* (3.11 ± 0.45) and

gcgrb^{vu601}/*gcgrb*^{vu610}*; Tg(gcga:GFP)* (2.75 ± 0.45) fish, although the difference was not statistically significant (Figure 5). These data suggest that the supernumerary α-cells are partially due to replication.

Mild hypoglycemia and hyperglucagonemia in glucagon receptor deficient zebrafish

To assess whether supernumerary α-cells in glucagon receptor deficient zebrafish contributes to hyperglucagonemia, we determined the mRNA and protein levels of glucagon at 7 dpf. Compared to wild-type controls, the levels of *gcga* and *gcgb* mRNA were both significantly increased in *gcgra*^{vu600}/*gcgra*^{vu600} and *gcgra*^{vu600}/*gcgra*^{vu600}*; gcgrb*^{vu601}/*gcgrb*^{vu601} larvae, but not in *gcgrb*^{vu601}/*gcgrb*^{vu601} larvae (Figure 6A and 6B). No change in insulin expression was detected (Figure 6C). Expression analysis by in situ hybridization confirmed an increase of *gcga* and *gcgb* in the islet of the double mutants (Supplemental Fig 2). The analysis also indicated elevated intestinal expression of the *preproglucagon* mRNA in the double mutants (Supplemental Fig 2), suggesting increased Glp-1 in the zebrafish mutants as in GCGR−/− mice (Gelling et al. 2003). To determine whether the increase of *gaca* and *gcgb* mRNA in the islet resulted in more glucagon peptide, we measured the total glucagon content using radioimmunoassay (RIA). Compared to total glucagon in the control group (3.23 ± 0.30 pg per fish), *gcgra*^{vu600}/*gcgra*^{vu600} (4.07 ± 0.16 pg, $P<0.05$) and *gcgra*^{vu600}/*gcgra*^{vu600}*; gcgrb*^{vu601}/*gcgrb*^{vu601} (5.83 ± 0.35pg, $P<0.001$) had more glucagon per fish (Figure 6D). The increased glucagon content was consistent with an increased α-cell number in the mutants.

To assess the effect of glucagon receptor deficiency on gluconeogenesis, we measured free glucose levels at 7 dpf. Compared to wild-type control, there was a significant decrease in *gcgra*^{vu600}/*gcgra*^{vu600}, *gcgrb*^{vu601}/*gcgrb*^{vu601} and *gcgra*^{vu600}/*gcgra*^{vu600}*; gcgrb*^{vu601}/*gcgrb*^{vu601} mutants (Fig. 5E). To determine whether this is due to changes in the expression of gluconeogenic genes, we measured the expression of *phosphoenolpyruvate carboxykinase* (soluble) (*pck1*), *phosphoenolpyruvate carboxykinase 2* (mitochondrial) (*pck2*), *glucose-6-phosphatase* (*g6pca.1*) mRNA by qRT-PCR (Figure 6F–6H). Compared to wild-type control, there was a significant reduction of *pck1, pck2* and *g6pca.1* mRNA levels in *gcgra*^{vu600}/*gcgra*^{vu600}*; gcgrb*^{vu601}/*gcgrb*^{vu601} larvae (Figure 6F–6H). However, no significant change in *pck1* and *g6pca.1* expression was found in *gcgra*^{vu600}/*gcgra*^{vu600} fish.

Discussion

Antagonism of glucagon action is a potential therapeutic approach in type 2 diabetes. To advance glucagon antagonism as a therapy requires a thorough understanding of its compensatory responses to such as α-cell hyperplasia. However, the molecular explanation for the α-cell hyperplasia is unknown. In an effort to identify the responsible factor or factors, we have used the genetic tractability of zebrafish to determine if the underlying compensatory mechanism is conserved. In this study, we characterize the glucagon receptors of zebrafish and demonstrate that α-cell hyperplasia occurs in zebrafish, like in rodents and humans, when glucagon receptor signaling is interrupted.

We show that the zebrafish have two glucagon receptor genes and that both are functional. This is likely due to the additional round of genome duplication in the teleost lineage

(Venkatesh 2003). As with many other gene duplications, *gcgra* and *gcgrb* are likely preserved because of functional partitioning: while both are expression in the liver and brain, *gcgra* is not expressed in intestines whereas *gcgrb* is not expressed in heart and muscle (Figure 2B). Nevertheless, their protein products respond similarly to both zebrafish glucagon peptides, Gcga and Gcgb, and couple to Gs to increase intracellular cAMP. An interesting pharmacological difference between the two receptors is that Gcgra is much less responsive to mammalian glucagon than Gcgrb. A surprising finding is that both zebrafish glucagon peptides fail to activate mouse GCGR (Figure 2E). This is similar to goldfish glucagon, which fails to bind rat GCGR (Chow, et al. 2004).

We show that glucagon receptor-deficient zebrafish display many phenotypes similar to Gcgr-deficient mice, having lower free glucose content and higher glucagon content, similar to the hypoglycemia and hyperglucagonemia seen in mice (Gelling et al. 2003; Vuguin, et al. 2006). Importantly, glucagon-receptor deficient zebrafish have a greater α-cell mass (Figure 4) and the increase of α-cells is at least partially from α-cell replication (Figure 5). Similar to our results, Ye et. al. reported that knockdown of zebrafish *gcga* by morpholino resulted in supernumerary α-cells partially from proliferation of existing α-cells.(Ye, et al. 2015). These data indicate that the compensatory mechanism to glucagon deficiency or interruption of glucagon signaling is conserved in zebrafish. In glucagon receptor-deficient mice, increased α-cell number is observed as early as day e15 (Vuguin et al. 2006). Similarly, the α-cell hyperplasia phenotype is very robust as early as 7 dpf in zebrafish, a stage that is amenable for large-scale genetic and small molecule screens. Therefore, glucagon receptor-deficient zebrafish offer an opportunity to unravel the molecular mechanism of compensatory α-cell hyperplasia resulting from glucagon antagonism and to discover other signals that regulate α-cell mass.

Supplementary Material

Refer to Web version on PubMed Central for supplementary material.

Acknowledgments

Funding

This work was supported by grants from the American Diabetes Association (1-13-BS-027 to WC), the NIH (DK088686 and GM110311 to WC, DK72473, DK89572, DK89538, DK104211, DK66636, and DK69603 to ACP), by a Merit Review Grant from the Department of Veterans Affairs (to ACP), USDA (AFRI 2014-04938 to WC), and by the Vanderbilt Diabetes Research and Training Center (DK20593) and JDRF (5-2013-111 to ACP and 3-PDF-2014-189-A-N to EDD). We utilized the Islet Analysis and Procurement Core of the Vanderbilt Diabetes Research and Training Center (DK02593). Confocal imaging was performed in the VUMC Cell Imaging Shared Resource (supported by NIH grants CA68485, DK20593, DK58404, HD15052, DK59637, and EY08126).

We thank Anastasia Coldren, Chunhua Dai, and members of the Chen lab for constructive discussions, and Amanda Goodrich and Corey Guthrie for excellent fish care.

References

Abrahamsen N, Lundgren K, Nishimura E. Regulation of glucagon receptor mRNA in cultured primary rat hepatocytes by glucose and cAMP. J Biol Chem. 1995; 270:15853–15857. [PubMed: 7541048]

Ali S, Drucker DJ. Benefits and limitations of reducing glucagon action for the treatment of type 2 diabetes. Am J Physiol Endocrinol Metab. 2009; 296:E415–421. [PubMed: 19116373]

Argenton F, Zecchin E, Bortolussi M. Early appearance of pancreatic hormone-expressing cells in the zebrafish embryo. Mech Dev. 1999; 87:217–221. [PubMed: 10495291]

Biemar F, Argenton F, Schmidtke R, Epperlein S, Peers B, Driever W. Pancreas development in zebrafish: early dispersed appearance of endocrine hormone expressing cells and their convergence to form the definitive islet. Dev Biol. 2001; 230:189–203. [PubMed: 11161572]

Brubaker PL, Drucker DJ. Structure-function of the glucagon receptor family of G protein-coupled receptors: the glucagon, GIP, GLP-1, and GLP-2 receptors. Receptors Channels. 2002; 8:179–188. [PubMed: 12529935]

Cermak T, Doyle EL, Christian M, Wang L, Zhang Y, Schmidt C, Baller JA, Somia NV, Bogdanove AJ, Voytas DF. Efficient design and assembly of custom TALEN and other TAL effector-based constructs for DNA targeting. Nucleic Acids Res. 2011; 39:e82. [PubMed: 21493687]

Chen M, Gavrilova O, Zhao WQ, Nguyen A, Lorenzo J, Shen L, Nackers L, Pack S, Jou W, Weinstein LS. Increased glucose tolerance and reduced adiposity in the absence of fasting hypoglycemia in mice with liver-specific Gs alpha deficiency. J Clin Invest. 2005; 115:3217–3227. [PubMed: 16239968]

Chow BK, Moon TW, Hoo RL, Yeung CM, Muller M, Christos PJ, Mojsov S. Identification and characterization of a glucagon receptor from the goldfish Carassius auratus: implications for the evolution of the ligand specificity of glucagon receptors in vertebrates. Endocrinology. 2004; 145:3273–3288. [PubMed: 15033912]

Conarello SL, Jiang G, Mu J, Li Z, Woods J, Zycband E, Ronan J, Liu F, Roy RS, Zhu L, et al. Glucagon receptor knockout mice are resistant to diet-induced obesity and streptozotocin-mediated beta cell loss and hyperglycaemia. Diabetologia. 2007; 50:142–150. [PubMed: 17131145]

Cruz SA, Tseng YC, Kaiya H, Hwang PP. Ghrelin affects carbohydrate-glycogen metabolism via insulin inhibition and glucagon stimulation in the zebrafish (Danio rerio) brain. Comp Biochem Physiol A Mol Integr Physiol. 2010; 156:190–200. [PubMed: 20138234]

Field HA, Dong PD, Beis D, Stainier DY. Formation of the digestive system in zebrafish. II. Pancreas morphogenesis. Dev Biol. 2003; 261:197–208. [PubMed: 12941629]

Gelling RW, Du XQ, Dichmann DS, Romer J, Huang H, Cui L, Obici S, Tang B, Holst JJ, Fledelius C, et al. Lower blood glucose, hyperglucagonemia, and pancreatic alpha cell hyperplasia in glucagon receptor knockout mice. Proc Natl Acad Sci U S A. 2003; 100:1438–1443. [PubMed: 12552113]

Hansen LH, Abrahamsen N, Nishimura E. Glucagon receptor mRNA distribution in rat tissues. Peptides. 1995; 16:1163–1166. [PubMed: 8532603]

Hesselson D, Anderson RM, Stainier DY. Suppression of Ptf1a activity induces acinar-to-endocrine conversion. Curr Biol. 2011; 21:712–717. [PubMed: 21497092]

Jiang G, Zhang BB. Glucagon and regulation of glucose metabolism. Am J Physiol Endocrinol Metab. 2003; 284:E671–678. [PubMed: 12626323]

Kedees MH, Grigoryan M, Guz Y, Teitelman G. Differential expression of glucagon and glucagon-like peptide 1 receptors in mouse pancreatic alpha and beta cells in two models of alpha cell hyperplasia. Mol Cell Endocrinol. 2009; 311:69–76. [PubMed: 19647035]

Kimmel CB, Ballard WW, Kimmel SR, Ullmann B, Schilling TF. Stages of embryonic development of the zebrafish. Dev Dyn. 1995; 203:253–310. [PubMed: 8589427]

Lee Y, Wang MY, Du XQ, Charron MJ, Unger RH. Glucagon receptor knockout prevents insulin-deficient type 1 diabetes in mice. Diabetes. 2011; 60:391–397. [PubMed: 21270251]

Li M, Maddison LA, Crees Z, Chen W. Targeted overexpression of CKI-insensitive cyclin-dependent kinase 4 increases functional beta-cell number through enhanced self-replication in zebrafish. Zebrafish. 2013; 10:170–176. [PubMed: 23544990]

Li M, Maddison LA, Page-McCaw P, Chen W. Overnutrition induces beta-cell differentiation through prolonged activation of beta-cells in zebrafish larvae. Am J Physiol Endocrinol Metab. 2014; 306:E799–807. [PubMed: 24473439]

Lieschke GJ, Currie PD. Animal models of human disease: zebrafish swim into view. Nat Rev Genet. 2007; 8:353–367. [PubMed: 17440532]

Livak KJ, Schmittgen TD. Analysis of relative gene expression data using real-time quantitative PCR and the 2(−Delta Delta C(T)) Method. Methods. 2001; 25:402–408. [PubMed: 11846609]

Longuet C, Robledo AM, Dean ED, Dai C, Ali S, McGuinness I, de Chavez V, Vuguin PM, Charron MJ, Powers AC, et al. Liver-specific disruption of the murine glucagon receptor produces alpha-cell hyperplasia: evidence for a circulating alpha-cell growth factor. Diabetes. 2013; 62:1196–1205. [PubMed: 23160527]

Lund A, Bagger JI, Christensen M, Knop FK, Vilsboll T. Glucagon and type 2 diabetes: the return of the alpha cell. Curr Diab Rep. 2014; 14:555. [PubMed: 25344790]

Maddison LA, Chen W. Nutrient excess stimulates beta-cell neogenesis in zebrafish. Diabetes. 2012; 61:2517–2524. [PubMed: 22721970]

Mayo KE, Miller LJ, Bataille D, Dalle S, Goke B, Thorens B, Drucker DJ. International Union of Pharmacology. XXXV. The glucagon receptor family. Pharmacol Rev. 2003; 55:167–194. [PubMed: 12615957]

Ni TT, Lu J, Zhu M, Maddison LA, Boyd KL, Huskey L, Ju B, Hesselson D, Zhong TP, Page-McCaw PS, et al. Conditional control of gene function by an invertible gene trap in zebrafish. Proc Natl Acad Sci U S A. 2012; 109:15389–15394. [PubMed: 22908272]

Venkatesh B. Evolution and diversity of fish genomes. Curr Opin Genet Dev. 2003; 13:588–592. [PubMed: 14638319]

Vuguin PM, Kedees MH, Cui L, Guz Y, Gelling RW, Nejathaim M, Charron MJ, Teitelman G. Ablation of the glucagon receptor gene increases fetal lethality and produces alterations in islet development and maturation. Endocrinology. 2006; 147:3995–4006. [PubMed: 16627579]

Ye L, Robertson MA, Hesselson D, Stainier DY, Anderson RM. Glucagon is essential for alpha cell transdifferentiation and beta cell neogenesis. Development. 2015; 142:1407–1417. [PubMed: 25852199]

Yu R, Dhall D, Nissen NN, Zhou C, Ren SG. Pancreatic neuroendocrine tumors in glucagon receptor-deficient mice. PLoS One. 2011; 6:e23397. [PubMed: 21853126]

Zecchin E, Filippi A, Biemar F, Tiso N, Pauls S, Ellertsdottir E, Gnugge L, Bortolussi M, Driever W, Argenton F. Distinct delta and jagged genes control sequential segregation of pancreatic cell types from precursor pools in zebrafish. Dev Biol. 2007; 301:192–204. [PubMed: 17059815]

Zhou C, Dhall D, Nissen NN, Chen CR, Yu R. Homozygous P86S mutation of the human glucagon receptor is associated with hyperglucagonemia, alpha cell hyperplasia, and islet cell tumor. Pancreas. 2009; 38:941–946. [PubMed: 19657311]

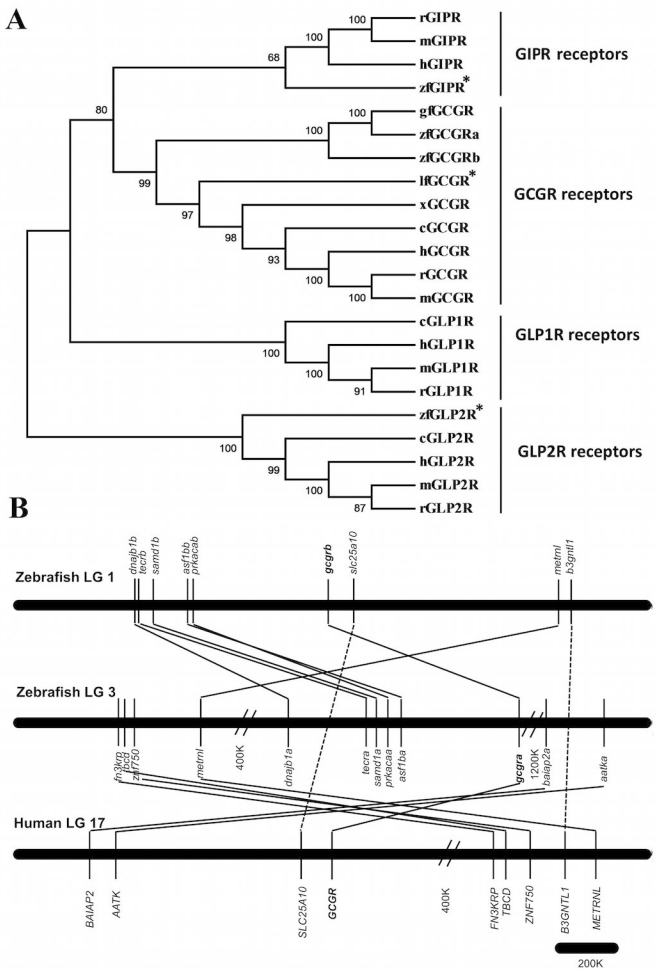

Figure 1. Identification of zebrafish *gcgra* and *gcgrb*

(A) Phylogenetic analysis of glucagon receptors. Full-length amino acid sequences of various receptors for glucagon-like peptides were analyzed using the neighbor-joining method. Posterior probability values (1,000 runs) for branches of the tree are given on nodes. GIPR = glucose-dependent insulinotropic polypeptide receptor; GLP1R, glucagon-like peptide 1 receptor; GLP2R, glucagon-like peptide 2 receptor. The prefixes used are: h, human; m, mouse; r, rat; c, chicken; x, Xenopus laevis; zf, zebrafish; gf, goldfish; lf, lungfish. *, predicted sequences. (B) Conserved synteny of *gcgra* and *gcgrb* to human *GCGR*. Zebrafish *gcgra* and *gcgrb* are located on Chromosome 3 and Chromosome 1, respectively. They share several syntenic genes of human *GCGR* on Chromosome 17.

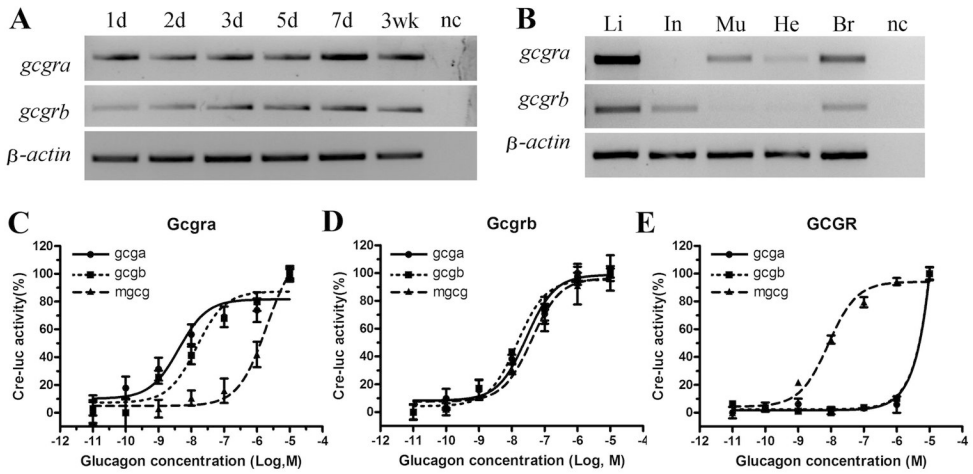

Figure 2. Expression patterns of *gcgra* and *gcgrb* and pharmacological profiles of their gene products

(A) RT-PCR analysis *gcgra* and *gcgrb* mRNA at different stages of development. The upper panel is *gcgra* mRNA, the middle panel is *gcgrb* mRNA and lower panel is *β-actin* mRNA. The developmental stages are shown at the top as days (d) or weeks (wk) post fertilization. nc, negative control. (B) RT-PCR analysis *gcgra* and *gcgrb* mRNA in different tissues in adult fish. Total RNA was isolated from Liver (Li), intestine (In), muscle (Mu), heart (He) and brain (Br) from adult zebrafish. nc, negative control. (C–E), Dose-response curves of zebrafish and mouse glucagon receptors to zebrafish and mouse glucagon peptides as measured by cAMP-dependent CRE-luciferase expression. HEK293T cells were co-transfected with pCRE-luc and expression vector pcDNA3.1(+) containing zebrafish glucagon receptor-a (Gcgra) (C), zebrafish glucagon receptor-b (Gcgrb) (D) and mouse glucagon receptor (GCGR) (E). The cells were exposed to different concentrations of zebrafish glucagon-a (Gcga), glucagon-b (Gcgb) and mouse glucagon (mGCG) peptides 48 hours after transient transfection. Each data point is the mean of triplicates.

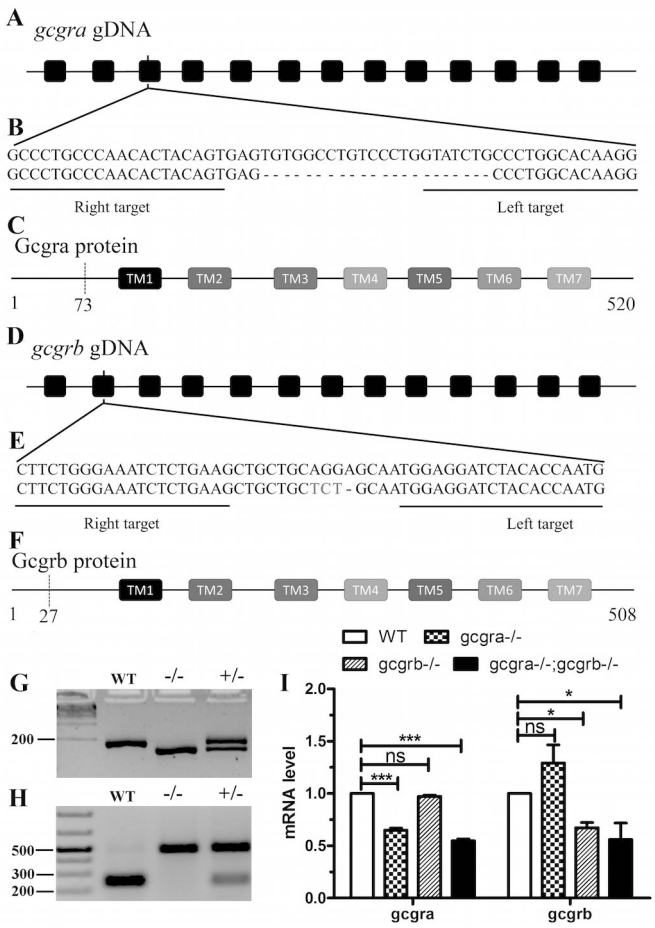

Figure 3. Generation of *gcgra*^{VU600} and *gcgrb*^{VU601}

(A–F) Schematic representations of TALEN targets and mutant alleles. Both *gcgra* (A) and *gcgrb* (D) consists of 13 exons (filled box). The TALEN pairs target exon 3 and exon 2, respectively. The sequences of the target regions are aligned to the selected alleles for *gcgra* (B) and *gcgrb* (E). The location of the truncation in the mutant gene product for *gcgra* (C) or *gcgrb* (F) are indicated with a dotted line. (G–H) Genotyping of wild, heterozygous and homozygous of *gcgra* (G) and *gcgrb* (H). (I). Real-time PCR analysis of *gcgra* and *gcgrb* mRNA levels. The results were from three independent experiments. All the values shown are means ± S.E., * P<0.05, *** P<0.001 by One-way ANOVA.

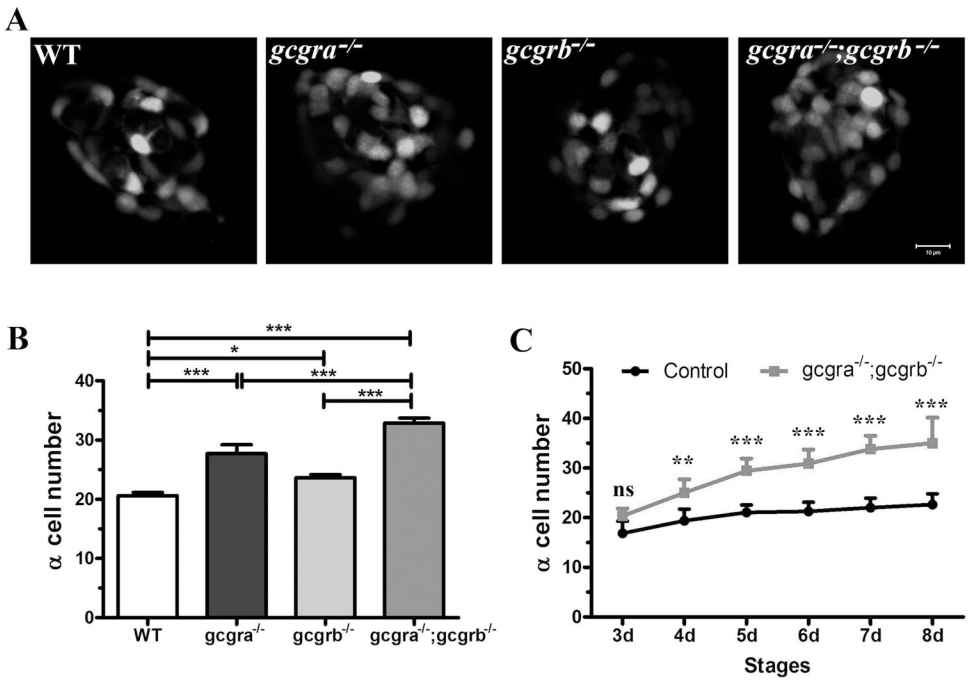

Figure 4. Homozygous mutants of *gcgr* genes develop α-cell hyperplasia

(A), Representative images of the principal islet of *Tg(gcga:GFP)*, *gcgra−/−;Tg(gcga:GFP)*, *gcgrb−/−;Tg(gcga:GFP)*, *gcgra−/−;gcgrb−/−;Tg(gcga:GFP)* at 7 dpf. The images are confocal projections; scale bars indicate 10μm. (B), Quantification of the α-cell number in different genotypes of zebrafish at 7 dpf. N=8–12. ** $P<0.01$, *** $P<0.001$ by One-way ANOVA. (C), α-cell number in *Tg(gcga:GFP)*, and *gcgra−/−;gcgrb−/−;Tg(gcga:GFP)* from 3 dpf to 8 dpf. n=8–16. The values shown are means ± S.E., ** $P<0.01$, *** $P<0.001$ by t-test.

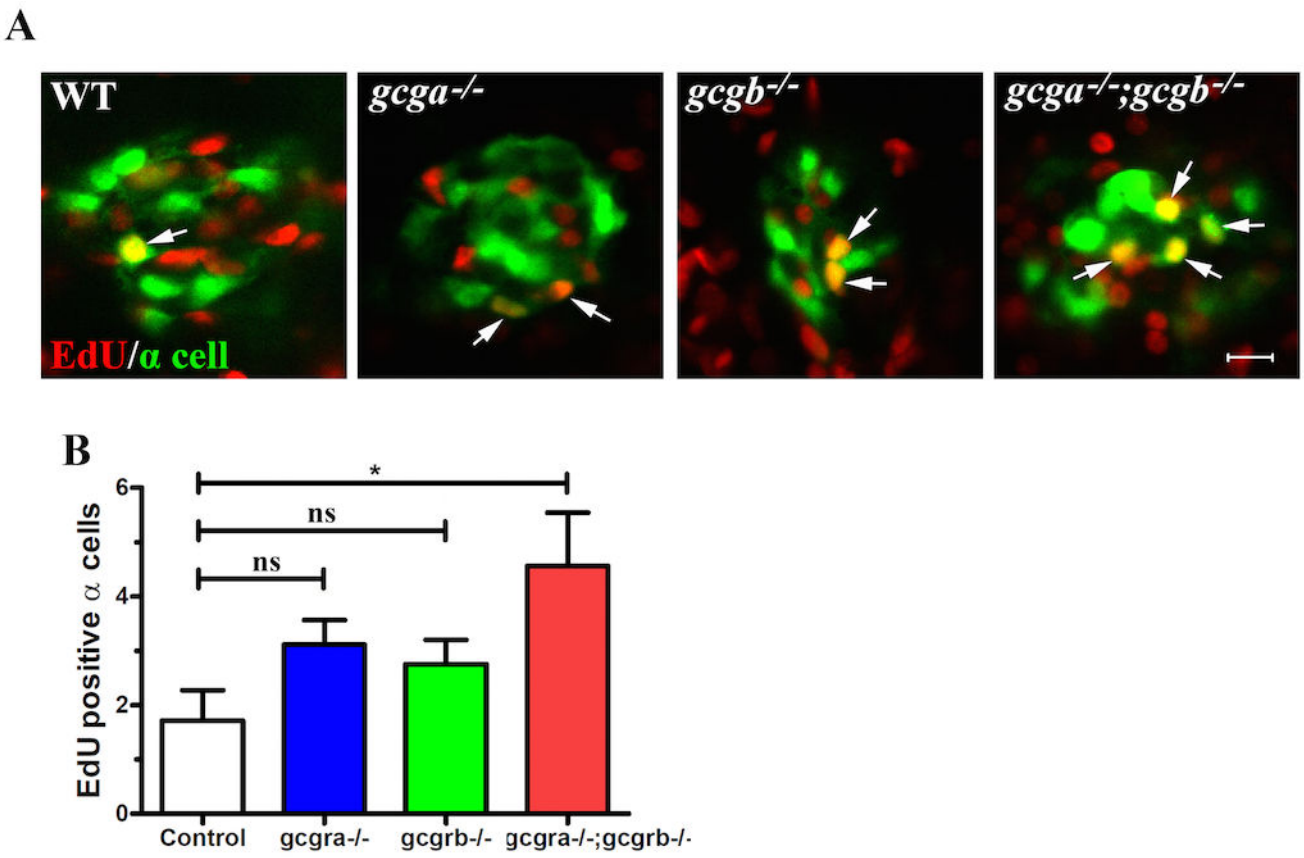

Figure 5. Increased α-cell proliferation in *gcgr*-deficient zebrafish larvae

(A). Representative images of different genotypes larvae by EdU staining. Arrows indicated the EdU (red) positive α-cell (green). The images are confocal projections; scale bar indicates 10 μm. (B). Quantification of EdU labeled α-cells. n= 7–10. All the values shown are means ± S.E., * $P<0.05$ by One-way ANOVA.

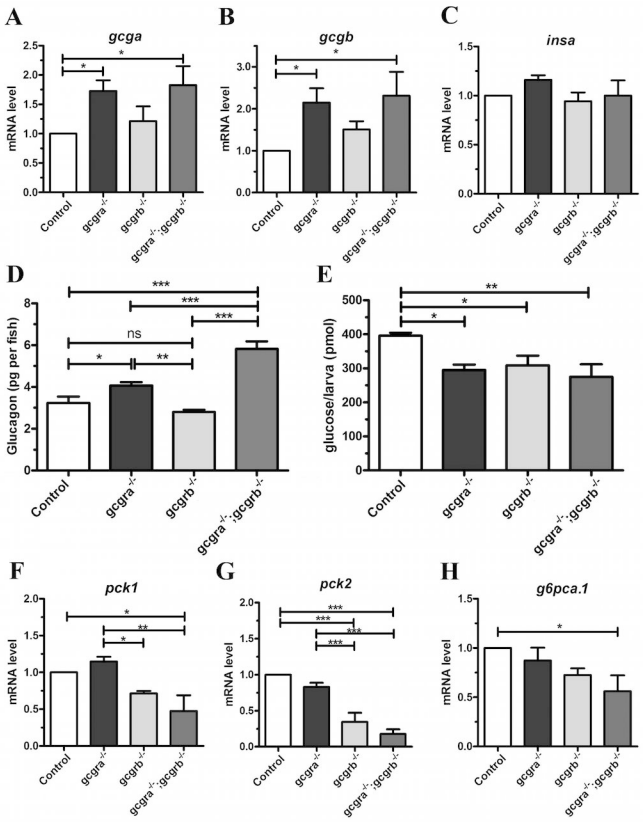

Figure 6. Defects in glucose metabolism in *gcgr*-deficient zebrafish at 7 dpf

(A–C). Real-time PCR analysis of *gcga* (A), *gcgb* (B), and insulin (C) mRNA in wildtype and mutant fish. (D). Total glucagon content in wildtype and mutant fish. (E). Total free glucose content in wildtype and mutant fish. (F–H) Quantitative RT-PCR analysis of the expression of key gluconeogenic genes *pck1* (F), *pck2*(G) and *g6pca.1* (H). Expression of β-actin was used as an internal control for all real-time PCR experiments. All the values shown are means ± S.E. from three independent experiments. * $P<0.05$, ** $P<0.01$, *** $P<0.001$ by One-way ANOVA.

Table 1

EC50 of glucagons to glucagon receptors as measured by cAMP-mediated luciferase activity.

	Gcga	Gcgb	mGCG
Gcgra	4.161e-009 (1.125e-009~1.539e-008)	1.461e-008 (5.827e-009 ~ 3.664e-008)	1.962e-006 (8.530e-007 ~ 4.513e-006)
Gcgrb	2.798e-008 (1.354e-008~5.779e-008)	1.488e-008 (8.770e-009~2.524e-008)	4.046e-008 (1.562e-008~1.048e-007)
mGCGR	~ 0.03148	~ 0.02404	8.329e-009 (5.481e-009 to 1.266e-008)

EC50 values, represent glucagon concentrations that elicit 50% of the maximum response to glucagon receptors. EC50 (upper panel in each cell) and 95% confidence intervals (lower panel in each cell) were shown. Each data point was the average of triplicates.